

# Nonclassical Rotational Inertia in Helium Crystals

A. C. Clark,\* J. T. West, and M. H. W. Chan

*Department of Physics, The Pennsylvania State University, University Park, Pennsylvania 16802*

(Dated: October 30, 2018)

It has been proposed that the observed nonclassical rotational inertia (NCRI) in solid helium results from the superflow of thin liquid films along interconnected grain boundaries within the sample. We have carried out new torsional oscillator measurements on large helium crystals grown under constant temperature and pressure. We observe NCRI in all samples, indicating that the phenomenon cannot be explained by a superfluid film flowing along grain boundaries.

PACS numbers: 67.80.-s, 61.72.Mm, 61.72.Lk

The finding of NCRI in solid helium [1] has been replicated in torsional oscillator (TO) measurements in four other laboratories [2, 3, 4]. The temperature dependence of NCRI, characterized by saturation in the low temperature limit and a gradual decay to zero at higher temperature, is qualitatively reproducible in all measurements. However, the onset temperature  $T_O$ , the point where NCRI becomes resolvable from the noise, varies between 150 mK and 400 mK in the studies of commercially pure helium ( $\sim 300$  ppb of  $^3\text{He}$ ). In addition, relative to the total amount of  $^4\text{He}$  in the cell the NCRI fraction (NCRIF) measured in the low temperature limit ranges from as little as 0.03% up to 20% [5]. In a large, cubic cell with linear dimensions of  $\sim 1$  cm, Rittner and Reppey found the measured NCRIF  $\approx 0.5\%$  could be reduced to  $< 0.05\%$  after annealing the sample [2]. Although this appears consistent with two numerical simulations in which perfect crystals are insulating [6], less dramatic results have been observed in similar annealing studies [3, 7, 8].

Although the presence of crystalline defects influences NCRIF, neither the specific defects of importance, nor their relationship with NCRI are known. Three fundamentally different kinds of defects that are present in solid helium are point defects such as vacancies or interstitials, dislocation lines, and grain boundaries. Vacancies, which are likely more prevalent than interstitials, were suggested to facilitate supersolidity in early theoretical literature [9]. Although recent investigations [10] report attractive forces between them, a small concentration of zero-point vacancies may still exist and facilitate NCRI [11]. However, it is impossible that they alone can account for an NCRIF of 20% [5].

There is an alternative model [12] in which NCRI actually results from superfluid liquid  $^4\text{He}$  flowing along grain boundaries. To be consistent with what is known of thin superfluid films [13], the  $\sim 200$  mK transition temperature implies an effective thickness of 0.06 nm (one-fifth of a monolayer). Thus, enormous surface areas of completely interconnected grain boundaries are necessary to support a supercurrent constituting even just one percent of the entire sample volume. This would require the crystallites to have an average grain size of  $\sim 20$  nm. Even for NCRIF = 0.03% [5, 8] the average grain size

would be  $< 1 \mu\text{m}$ , whereas samples grown by the blocked capillary (BC) method commonly result in crystals with linear dimensions  $\geq 0.1$  mm, as determined by thermal conductivities [14] and x-ray diffraction [15]. In addition, annealing is found to increase this value [14]. The same BC method was used in all previous TO studies, and involves filling the sample cell through the hollow torsion rod with high pressure liquid helium, freezing a section of  $^4\text{He}$  in the filling line (the block), and then cooling the constant volume below the block along the solid-liquid coexistence boundary until solidification is complete.

Two growth techniques that are superior to the BC method [16, 17] are carried out at a fixed point anywhere on the solid-liquid coexistence curve. The first, constant pressure (CP) growth, is achieved by slowly cooling the cell while a specific freezing pressure  $P_F$  is maintained. The second, constant temperature (CT) growth, takes place at a single freezing temperature  $T_F$  for minimal overpressures above  $P_F$ . The latter technique is most often (as it is in this study) employed when growing low pressure solids from the superfluid phase [16, 17]. The first extensive investigations demonstrating that large single crystals are reliably grown at CP/CT combined either *in situ* x-ray diffraction [18] or optical birefringence [19, 20] techniques with sound velocity measurements. An important experimental detail from Ref.'s [17, 18, 19, 20] is that the  $^4\text{He}$  filling line necessarily remained open during solidification. Also, a cold surface at one end of the cell seeded crystals, whereas the remaining surfaces were poor thermal conductors so as to avoid the nucleation of multiple crystallites. Due to such reliability, very similar methods have been incorporated in all studies of  $^4\text{He}$  single crystals since the early 1970s.

The motivation of the present work was to carry out a definitive experiment to test the grain boundary model. In an effort to separate the effects of isotopic impurities [8], samples were grown from both “isotopically pure”  $^4\text{He}$  ( $\sim 1$  ppb of  $^3\text{He}$ ) and commercially pure  $^4\text{He}$  ( $\sim 300$  ppb of  $^3\text{He}$ ). Measurements have been carried out in two torsional oscillators, one made from beryllium copper (BeCu) and one from coin silver (AgCu) (see Fig. 1a). Unlike other TO's in which a hollow torsion rod serves as the  $^4\text{He}$  filling line [1, 2, 3, 4, 5, 7, 8], the torsion rod

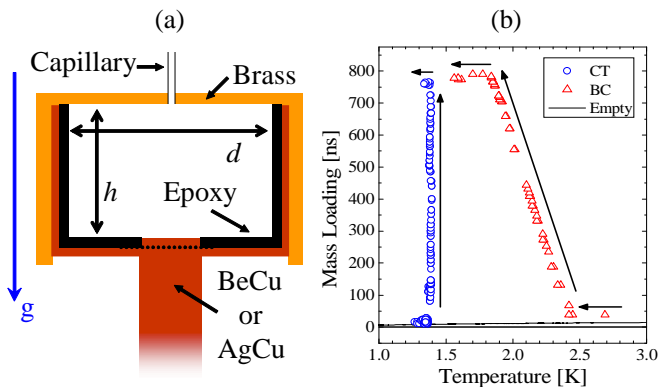


FIG. 1: (a) Schematic drawing of TO's. The epoxy coating is 0.025 cm thick on the bottom of each cell, and 0.05/0.04 cm thick on the BeCu/AgCu walls. The 0.25 cm diameter BeCu cold spot is recessed (to the dotted line) from the epoxy layer. In the AgCu TO the cold surface is flush with the epoxy layer. Some relevant parameters for the BeCu/AgCu TO are  $h = 0.483/0.597$  cm,  $d = 0.914/1.016$  cm,  $\tau = 0.933/1.27$  ms (resonant period at 20 mK). (b) Mass loading of BeCu TO during growth of two samples. The minimum loading (solid at 25 bar) of the BeCu/AgCu TO is 740/2000 ns.

is solid and a CuNi capillary (o.d. = 0.3 mm, i.d. = 0.1 mm) was soldered to the opposite end of the cell. Apart from a small cold spot from which to seed crystals, the walls are coated with a thin layer of epoxy. This design allows us to seed the crystal at the cell bottom and maintain an open filling line during freezing, and thus enabled the growth of crystals at CT/CP within a TO for the first time. Having replicated the precise conditions outlined in Ref.'s [17, 18, 19, 20], we can be confident that many of our samples are single crystals or at worst comprised of just a few large crystals in the sample cell. We note that the capillary can also be intentionally blocked with solid  $^4\text{He}$  during the growth of a crystal, mimicking the BC method employed in previous TO studies.

The mass loading of the BeCu TO during crystal formation is displayed in Fig. 1b for two representative samples, one grown at CT and one by BC. For the BC sample the molar volume  $V_M$  of the solid during growth ranges from  $19.3 \text{ cm}^3 \text{ mol}^{-1}$  (at  $T = 2.45$  K and  $P = 55$  bar) to  $20.7 \text{ cm}^3 \text{ mol}^{-1}$  ( $T = 1.8$  K and  $P = 30.7$  bar). In contrast to this 7% change in  $V_M$ , the sample grown at CT from the superfluid was subjected to variations in  $V_M$  of  $\sim 0.07\%$  (i.e., temperature variations of  $\sim 20$  mK).

The temperature dependence of NCRIF in a number of BC and CT/CP samples is shown in Fig. 2. For a particular cell the NCRIF in BC samples is larger than that in samples grown at CT/CP. This is true for both  $^3\text{He}$  concentrations. Further, we find that  $T_O$  is reduced when employing the CT/CP growth. Surprisingly, there is an order of magnitude difference in the NCRIF measured in the two cells. It appears that for both BC and CT/CP samples, NCRIF is very sensitive to the exact

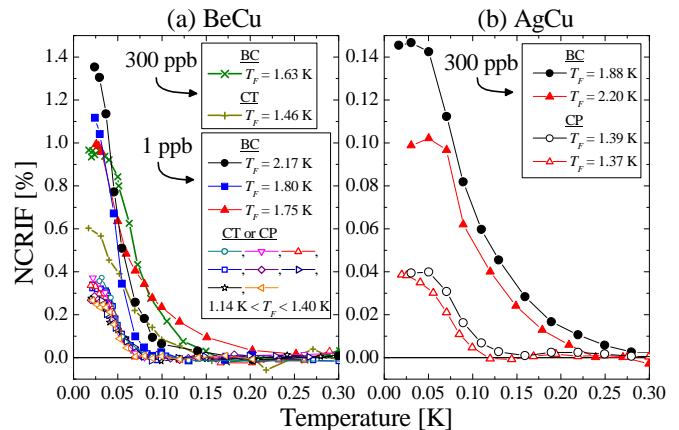


FIG. 2: (a) Comparison of several BC, CP, and CT samples grown in the BeCu TO with two different impurity levels.  $T_F$  is the temperature where solidification is complete. For eight 1 ppb crystals grown at CT/CP,  $0.26\% \leq \text{NCRIF} \leq 0.38\%$  ( $\pm 0.01\%$ ) and  $T_O = 79 \pm 5$  mK. Among 12 BC samples,  $0.46\% \leq \text{NCRIF} \leq 2.0\%$  and  $80 \text{ mK} \leq T_O \leq 275$  mK. The two 300 ppb samples grown in the BeCu TO are also shown. The maximum speed at the rim of the cell is  $< 5 \mu\text{m s}^{-1}$  in all cases. (b) The four 300 ppb samples grown in the AgCu TO. Rim speeds are  $< 8 \mu\text{m s}^{-1}$ .

internal geometry, construction materials, and thermal properties of the cells. For example, temperature gradients within the BeCu TO during growth are larger than in the AgCu TO due to the thicker epoxy layer and the much lower thermal conductivity of BeCu.

The most striking result from our study is that all eight 1 ppb samples that were grown at CT/CP (at a rate of  $\sim 1 \mu\text{m s}^{-1}$ ) collapse onto a single curve above 40 mK and thus share a common onset temperature. The vast improvement in reproducibility over that of BC samples is most likely due to the formation of single crystals within the cell. The spread in NCRIF at lower temperatures may be related to differences in crystalline defect (e.g., dislocations) densities.

We have carried out several annealing studies to investigate the defects in our crystals. For a BC sample (see Fig. 2b,  $T_F = 2.20$  K) in the AgCu TO we found NCRIF to interestingly increase from 0.1% to 0.2% upon repeated annealing. The dissipation, which accompanies NCRIF in the form of a peak [1], also increased. In the BeCu TO we found NCRIF in BC samples to decrease with annealing. The most dramatic reduction occurred in a 1 ppb sample grown with the BC method through the bcc-hcp phase boundary (see Fig. 3). The sizeable tail of NCRIF is such that  $T_O \approx 275$  mK. This was dramatically reduced following the first anneal at relatively low temperature. In fact, after 25 cumulative hours of annealing NCRIF asymptotically approaches that found in CT/CP samples. For a 1 ppb crystal freshly grown at CT there is no noticeable change in NCRIF even after 40 h of annealing.

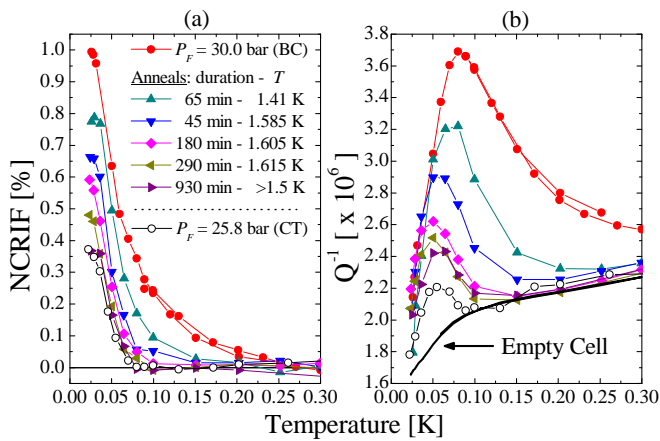


FIG. 3: (a) NCRIF after each sequential anneal for a BC sample quenched from the bcc phase. A CT crystal grown from the superfluid is potted for comparison. (b) Asymmetric reduction in  $Q^{-1}$  following each anneal. All data were obtained with rim speeds  $< 3 \mu\text{m s}^{-1}$ .

Annealing the BC sample in Fig. 3 also led to a dramatic reduction in the dissipation ( $\propto Q^{-1}$ ). Repeated heat treatments reduce the width of the peak, such that its position remains close to the temperature where NCRIF changes most rapidly. The fully annealed dissipation peak, just as NCRIF, approaches that found in CT/CP samples. A phenomenological model [21] associates the dissipation with a temperature dependent coupling between the superfluid and normal components of the solid, and predicts  $(|\Delta\tau|/\tau)/(\Delta Q^{-1}) \approx 1$  for a homogeneous sample ( $> 1$  indicates inhomogeneity). The ratio for this sample at different stages of annealing evolves nonmonotonically from 9.5 to 12 to 10.5.

When the results of the present set of measurements are considered together with the myriad of data from earlier studies [1, 2, 3, 4, 5, 7, 8], dislocations emerge as a likely important class of defects. Dislocation lines form an entangled web throughout each crystal, and can vary in density by more than five orders of magnitude ( $< 10^5 \text{ cm}^{-2}$  to  $10^{10} \text{ cm}^{-2}$ ) in solid helium samples grown above 1 K using different methods. The actual line density deduced from sound measurements [22] depends very sensitively (varying by four orders of magnitude) on the exact growth conditions of crystals [22, 23]. It also can vary by at least one order of magnitude from cell to cell, despite nearly identical growth procedures [22, 24]. The large range of line densities and their sensitivity to sample growth and containment can conceivably explain the very different NCRIF's observed, even for single crystals. It is also known that only some types of dislocations can be annealed away, which may explain the unreliable effectiveness of annealing on the reduction of NCRIF.

The quantum mechanical motion of a single dislocation has recently been considered [25], but a meaningful comparison with experiments requires a thorough analysis of

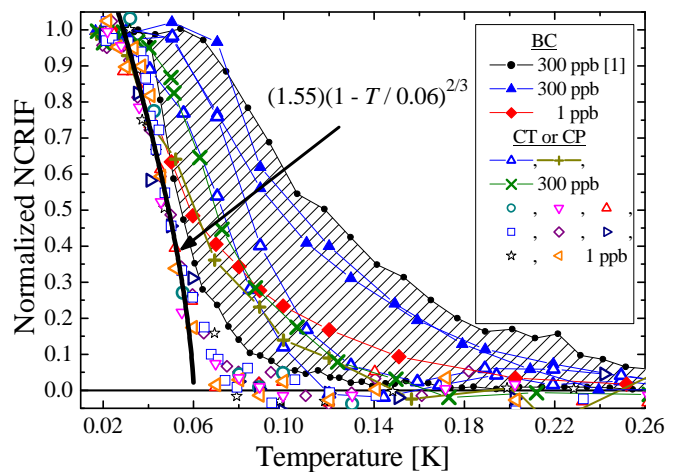


FIG. 4: Normalized NCRIF in various samples. There is a wide spread in the data from the original KC experiment [1]. BC samples presented in Fig. 2 possess a high temperature tail of NCRIF. CT/CP samples have a considerably sharper onset. A two-thirds power law is plotted for comparison.

complex dislocation networks. Recent simulations have shown that the core of some dislocations may support superflow [26]. Applying Luttinger liquid theory to the dislocation network, Ref. [26] predicts that if the dislocation cores alone are responsible for supersolidity then  $T_C \propto (\rho_S/\rho)^{0.5}$ . Upon comparing several samples in Fig. 2, the above relation is found not to be satisfied if we take  $T_C = T_O$  and  $\rho_S/\rho = \text{NCRIF}$ . It has also been proposed that  $^3\text{He}$  impurities nucleate and stabilize dislocations, which in turn produce a disordered supersolid phase by providing a flow path for  $^4\text{He}$  interstitials [27].

In addition to the magnitude of NCRIF, the high temperature tail and thus  $T_O$  are correlated with the way samples are prepared (see Fig. 2). Several points can be drawn from the data in Fig. 4, which are scaled by the low temperature NCRIF. First, the high temperature tail of NCRIF varies greatly for different BC samples, which are presumably polycrystalline. Second, the behavior of NCRIF in CT/CP samples is distinct in that the temperature dependence is much sharper, with a well-defined onset temperature. This is most apparent in crystals of 1 ppb purity. The addition of  $^3\text{He}$  broadens the transition and pushes the onset of NCRIF to higher temperature. The sensitivity to impurities confirms the general trends observed for a large number of BC samples that were studied over a wide range of  $^3\text{He}$  concentrations [8].

All the data in Fig. 4 were obtained at similar measurement frequencies. A recent TO measurement [4] on the same 300 ppb sample at two different frequencies found  $T_O \approx 250 \text{ mK}$  at 1173 Hz and  $T_O \approx 150 \text{ mK}$  at 496 Hz. They also report irreversible changes in NCRIF below  $\sim 40 \text{ mK}$  upon variation of the oscillation speed. We have investigated [28] the thermal history of what appears to be the same phenomenon in 1 ppb crystals

and find that in the low temperature limit there are in fact many metastable NCRIF's available to the system. These results, as well as previously observed critical velocities on the order of one quantum of circulation [7], indicate that the likely excitations in the system are vortices.

A recent model [29] capturing several aspects of the experiments equates NCRI to the rotational susceptibility of a vortex liquid phase. The high temperature tail of NCRI is said to reflect the finite response time of vortices in the sample, which are further slowed by  $^3\text{He}$  atoms dragged along with them. However, the low temperature behavior of NCRIF [4, 28] suggests that at least a portion of the vortices are pinned. Trace amounts of  $^3\text{He}$  are found to produce significant changes in the sound velocity and elastic constants measured in solid  $^4\text{He}$ . These results indicate that  $^3\text{He}$  impurities condense onto dislocation lines [30]. It is reasonable to assume that these  $^3\text{He}$ -rich regions are the vortex pinning sites within the sample. In this scenario the interplay between vortices, impurities, and dislocations greatly impact the measured NCRIF in the solid.

A broad heat capacity peak near 75 mK was recently detected in solid  $^4\text{He}$  [31]. This finding supports the notion that the appearance of NCRI is a genuine signature of the transition between the normal and supersolid phases. It is then natural to wonder if it falls into the same universality class as that of superfluid  $^4\text{He}$ , i.e., the 3D XY model. The gradual onset of NCRI previously observed is not consistent with this expectation. However, the sharp onset present in CT/CP crystals of 1 ppb purity is intriguing. We noted above that the NCRIF's in all eight samples collapse onto a single curve for  $T > 40$  mK (see Fig. 2). The NCRIF data of these crystals between 30 mK and 57 mK, as shown in Fig. 4, can be represented by the expected two-thirds power law, with a critical temperature  $T_C \approx 60$  mK. If this highly speculative "fit" is applicable then the tail between 60 mK and 79 mK is attributable to the finite measurement frequency, residual (1 ppb)  $^3\text{He}$  impurities, and crystalline defects. Measurements at a much lower frequency may reveal if there is any validity to this speculation.

To summarize, we have shown that NCRI is found in large crystals of solid  $^4\text{He}$  grown at constant CT/CP. In contrast to the results from BC samples, the temperature dependence of NCRI in what are very likely single crystals is reproducible and exhibits a sharp onset.

We thank P. W. Anderson, J. Beamish, W. F. Brinkman, D. A. Huse, E. Kim, H. Kojima, X. Lin, N. Mulders, J. D. Reppy, and A. S. C. Rittner for informative discussions. We also thank J. A. Lipa for the 1 ppb purity helium and J. D. Reppy for the thin capillary used in our cells. Support was provided by NSF Grants DMR 0207071 and 0706339.

- 
- \* Electronic address: acc172@psu.edu
- [1] E. Kim and M. H. W. Chan, *Science* **305**, 1941 (2004).
  - [2] A. S. C. Rittner and J. D. Reppy, *Phys. Rev. Lett.* **97**, 165301 (2006).
  - [3] A. Penzev, Y. Yasuta, and M. Kubota, *J. Low Temp. Phys.* **148**, 667 (2007); M. Kondo, S. Takada, Y. Shibayama, and K. Shirahama, *ibid.* **148**, 695 (2007).
  - [4] Y. Aoki, J. C. Graves, and H. Kojima, *Phys. Rev. Lett.* **99**, 015301 (2007).
  - [5] A. S. C. Rittner and J. D. Reppy, *Phys. Rev. Lett.* **98**, 175302 (2007).
  - [6] D. M. Ceperley and B. Bernu, *Phys. Rev. Lett.* **93**, 155303 (2004); N. V. Prokof'ev and B. V. Svistunov, *ibid.* **94**, 155302 (2005).
  - [7] E. Kim and M. H. W. Chan, *Phys. Rev. Lett.* **97**, 115302 (2006).
  - [8] E. Kim, J. S. Xia, J. T. West, X. Lin, and M. H. W. Chan, *Bull. Am. Phys. Soc.* **52**, 610 (2007).
  - [9] A. F. Andreev and I. M. Lifshitz, *Sov. Phys. JETP* **29**, 1107 (1969); G. V. Chester, *Phys. Rev. A* **2**, 256 (1970).
  - [10] M. Boninsegni *et al.*, *Phys. Rev. Lett.* **97**, 080401 (2006); G. D. Mahan and H. Shin, *Phys. Rev. B* **74**, 214502 (2006).
  - [11] D. E. Galli and L. Reatto, *Phys. Rev. Lett.* **96**, 165301 (2006).
  - [12] E. Burovski, E. Kozik, A. Kuklov, N. V. Prokof'ev, and B. V. Svistunov, *Phys. Rev. Lett.* **94**, 165301 (2005); S. Sasaki, R. Ishiguro, F. Caupin, H. J. Maris, and S. Balibar, *Science* **313**, 1098 (2006); *J. Low Temp. Phys.* **148**, 665 (2007); L. Pollet *et al.*, *Phys. Rev. Lett.* **98**, 135301 (2007).
  - [13] J. M. Kosterlitz and D. J. Thouless, *J. Phys. C: Solid State Phys.* **6**, 1181 (1973); D. J. Bishop and J. D. Reppy, *Phys. Rev. Lett.* **40**, 1727 (1978).
  - [14] F. J. Webb, K. R. Wilkinson, and J. Wilks, *Proc. R. Soc. A* **214**, 546 (1952); G. A. Armstrong, A. A. Helmy, and A. S. Greenberg, *Phys. Rev. B* **20**, 1061 (1979).
  - [15] A. F. Schuch and R. F. Mills, *Phys. Rev. Lett.* **8**, 469 (1962).
  - [16] J. E. Vos *et al.*, *Physica* **37**, 51 (1967).
  - [17] O. W. Heybey and D. M. Lee, *Phys. Rev. Lett.* **19**, 106 (1967).
  - [18] D. S. Greywall, *Phys. Rev. A* **3**, 2106 (1971).
  - [19] R. Wanner and J. P. Franck, *Phys. Rev. Lett.* **24**, 365 (1970).
  - [20] R. H. Crepeau, O. Heybey, D. M. Lee, and S. A. Strauss, *Phys. Rev. A* **3**, 1162 (1971).
  - [21] D. A. Huse and Z. U. Khandker, *Phys. Rev. B* **75**, 212504 (2007).
  - [22] R. Wanner, I. Iwasa, and S. Wales, *Solid State Commun.* **18**, 853 (1976).
  - [23] F. Tsuruoka and Y. Hiki, *Phys. Rev. B* **20**, 2702 (1979).
  - [24] I. Iwasa, K. Araki, and H. Suzuki, *J. Phys. Soc. Jpn.* **46**, 1119 (1979).
  - [25] P.-G. de Gennes, *C. R. Physique* **7**, 561 (2006).
  - [26] M. Boninsegni *et al.*, arXiv:0705.2967v1 (2007).
  - [27] E. Manousakis, *Europhys. Lett.* **78**, 36002 (2007).
  - [28] A. C. Clark and M. H. W. Chan, to be published.
  - [29] P. W. Anderson, *Nature Physics* **3**, 160 (2007).
  - [30] H. Suzuki and I. Iwasa, *J. Phys. Soc. Jpn.* **49**, 1722 (1980); M. A. Paalanen, D. J. Bishop, and H. W. Dail,

Phys. Rev. Lett. **46**, 664 (1981).

[31] X. Lin, A. C. Clark, and M. H. W. Chan, to be published.